

# A Dicobalt- $\mu$ -oxo Polyoxometalate Compound, $[(\alpha_2\text{-P}_2\text{W}_{17}\text{O}_{61}\text{-Co})_2\text{O}]^{14-}$ , – A Potent Species for Water Oxidation, C–H Bond Activation and Oxygen Transfer

Delina Barats-Damatov,<sup>a</sup> Linda J. W. Shimon,<sup>b</sup> Lev Weiner,<sup>b</sup> Roy Schreiber,<sup>a</sup> Pablo Jiménez-Lozano,<sup>c</sup> Josep M. Poble<sup>c</sup>, Coen de Graaf,<sup>c,d</sup> and Ronny Neumann<sup>a\*</sup>

(a) Department of Organic Chemistry, Weizmann Institute of Science, Rehovot, Israel 76100 (b) Chemical Research Support Unit, Weizmann Institute of Science, Rehovot, Israel, 76100 (c) Departament de Química Física i Inorgànica, Universitat Rovira i Virgili, 43007 Tarragona Spain (d) Institució Catalana de Recerca i Estudis Avançats (ICREA), Passeig Lluís Companys 23, 08010, Barcelona, Spain

**ABSTRACT:** High valent oxo compounds of transition metals are often implicated as active species in oxygenation of hydrocarbons through carbon-hydrogen bond activation or oxygen transfer and also in water oxidation. Recently, several examples of cobalt catalyzed water oxidation have been reported and cobalt(IV) species have been suggested as active intermediates. A reactive species, formally a dicobalt(IV)- $\mu$ -oxo polyoxometalate compound  $[(\alpha_2\text{-P}_2\text{W}_{17}\text{O}_{61}\text{Co})_2\text{O}]^{14-}$ ,  $[(\text{POMCo})_2\text{O}]$ , has now been isolated and characterized by the oxidation of a monomeric  $[\alpha_2\text{-P}_2\text{W}_{17}\text{O}_{61}\text{Co}^{\text{II}}(\text{H}_2\text{O})]^{8-}$ ,  $[\text{POMCo}^{\text{II}}\text{H}_2\text{O}]$ , with ozone in water. The crystal structure shows a nearly linear Co–O–Co moiety with a Co–O bond length of  $\sim 1.77$  Å. In aqueous solution  $[(\text{POMCo})_2\text{O}]$  was identified by  $^{31}\text{P}$  NMR, Raman and UV-vis spectroscopy. Reactivity studies showed that  $[(\text{POMCo})_2\text{O}]$  is an active compound for the oxidation of  $\text{H}_2\text{O}$  to  $\text{O}_2$ , direct oxygen transfer to water-soluble sulfoxides and phosphines; indirect epoxidation of alkenes via a Mn porphyrin, and the selective oxidation of alcohols by carbon-hydrogen bond activation. The latter appears to occur via a hydrogen atom transfer mechanism. Density functional and CASSCF calculations strongly indicate that the electronic structure of  $[(\text{POMCo})_2\text{O}]$  is best defined as a compound having two cobalt(III) atoms with two oxidized oxygen atoms.

## INTRODUCTION

In the biological world, the intermediacy of reactive oxo species of iron, copper and manganese metalloenzymes enables C–H bond activation of hydrocarbons by monooxygenase enzymes<sup>1</sup> and water oxidation by photosystem II.<sup>2</sup> Beyond the importance of understanding the mode of activity of these metalloenzymes there is intense interest in the development of synthetic catalysts for such transformations. Thus, the oxidation of gaseous methane to liquid methanol would aid in the utilization of huge natural gas reserves<sup>3</sup> and oxidation of water would enable formation of hydrogen gas as an alternative energy carrier.<sup>4</sup> Therefore, much research has been devoted to iron and copper-based catalysts for hydrocarbon oxidation<sup>5</sup> and mostly ruthenium and manganese-based catalysts, but also others for water oxidation.<sup>6</sup>

Cobalt salts and complexes have long been known to be active in hydrocarbon autooxidation reactions and for dioxygen coordination.<sup>7</sup> Their use in oxygen transfer reactions with oxygen donors that ostensibly form high valent Co–O intermediates has been only relatively scantily investigated,<sup>8</sup> and it has been proposed that terminal  $\text{Co}^{\text{IV}}$ -oxo species may be formed and active.<sup>9</sup> Recently, such a  $\text{Co}^{\text{IV}}$ -oxo species stabilized by  $\text{Sc}^{3+}$  has been reported,<sup>10</sup> although others have suggested that this may be a  $\text{Co}^{\text{III}}\text{OH}$  compound.<sup>11</sup> About thirty years ago, there were some reports on the use of aquo cobalt(II) for the oxidation of water to  $\text{O}_2$  with  $\text{Co}^{\text{IV}}$  species suggested as active intermediates.<sup>12</sup> This general area of research has been revitalized after Kanan and Nocera's publication five years ago and subsequent research on the high activity of a cobalt-phosphate cluster for water oxidation.<sup>13</sup> Since then, there has been a flurry of activity where cobalt containing compounds including molecular catalysts,<sup>14</sup> bioinspired “cubane” type compounds,<sup>15</sup> and various colloidal, cluster and nanoparticulate materials<sup>16</sup> have been used for water oxidation. In this context, anionic cobalt-containing polyoxometalates have also been suggested

as molecular water oxidation photocatalysts.<sup>17</sup> The stability of the catalysts under turnover conditions are being debated.<sup>18</sup>

Polyoxometalates also provide fascinating possibilities for the study of transition-metal reactivity with oxidants in a purely inorganic oxo-ligand environment and also in water.<sup>19</sup> They also allow stabilization of important intermediates otherwise not observable as shown in the isolation of Fe(III)-peroxo species upon addition of  $\text{O}_2$  to a hexasubstituted Fe(II) polyoxometalate.<sup>20</sup> Utilizing the intrinsic stability of polyoxometalate frameworks towards ozone, we have isolated a polyoxometalate based dimer containing a *formally*  $\text{Co}^{\text{IV}}\text{--O--Co}^{\text{IV}}$  moiety. The isolation of this compound and its spectroscopic characterization has allowed us to demonstrate that it is both a competent water oxidation species and is reactive for the selective C–H bond activation of water-soluble alcohols and oxygen transfer to sulfoxides. In the presence of a Mn(III)porphyrin, efficient oxygen transfer to alkenes was also demonstrated. Calculations show that the active compound is *not* a bis- $\text{Co}^{\text{IV}}$  species but rather it is better represented as a bis- $\text{Co}^{\text{III}}$  compound with two oxygen centered cation radicals or holes.

## RESULTS AND DISCUSSION

### Preparation and Characterization of Active Species

The experimental study was carried out using  $[\alpha_2\text{-P}_2\text{W}_{17}\text{O}_{61}\text{Co}^{\text{II}}(\text{H}_2\text{O})]^{8-}$   $[\text{POMCo}^{\text{II}}\text{H}_2\text{O}]$  with the Wells-Dawson structure as the polyoxoanion, Figure 1, and ozone as oxidant. The rationale behind these choices was that ozone is a strong, potentially two electron oxidant, known, by spectroscopic studies, to be able to form a  $\text{Fe}^{\text{IV}}\text{=O}$  species in water and thus was also a reasonable candidate for the formation of a  $\text{Co}^{\text{IV}}$  compound.<sup>21</sup> Furthermore, as has been shown in the past, polyoxometalates are typically water soluble and stable towards ozone.<sup>22</sup>  $[\text{POMCo}^{\text{II}}\text{H}_2\text{O}]$  has a specific advantage in that the two phosphorus atoms have different chemical envi-

ronments and this fact can effectively be utilized in  $^{31}\text{P}$  NMR studies for speciation in solution.<sup>23</sup>

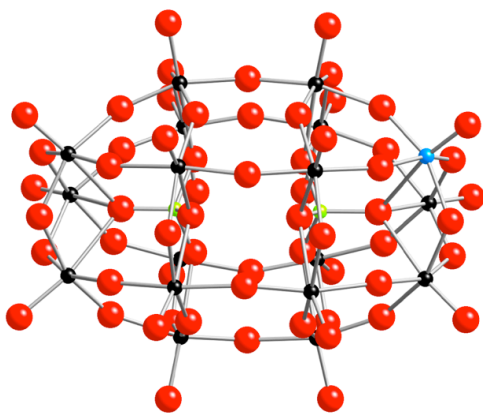


Figure 1. The ball and stick structural representation of  $[\text{POMCo}^{\text{II}}\text{H}_2\text{O}]$ . Solvent molecules and cations are not shown for clarity. P - green; W - black; O - red; Co - blue.

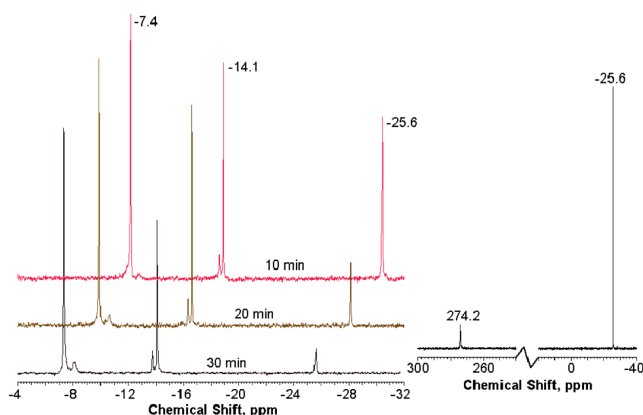


Figure 2.  $^{31}\text{P}$  NMR spectrum of 10 mM aqueous  $\text{K}[\text{POMCo}^{\text{II}}\text{H}_2\text{O}]$  at 22 °C (right) and changes upon ozonation as a function of time (left, where the peak at +274.2 ppm is not shown for convenience).

Thus, ozone (concentration - 25 mg/L, rate - 6.25 mg/min) dissolved in  $\text{O}_2$  was bubbled through a 10 mM aqueous solution of  $\text{K}_8[\alpha_2\text{-P}_2\text{W}_{17}\text{O}_{61}\text{Co}^{\text{II}}(\text{H}_2\text{O})]^{8-}$   $\text{K}[\text{POMCo}^{\text{II}}\text{H}_2\text{O}]$ , at  $\sim 0$  °C. After a few minutes the salmon pink solution began to become dark red (maroon) and the  $^{31}\text{P}$  NMR showed the formation of one new major species, Figure 2 left. The  $^{31}\text{P}$  NMR spectrum of  $\text{K}[\text{POMCo}^{\text{II}}\text{H}_2\text{O}]$  with a narrow peak at  $-25.6$  ppm and a broad peak at  $+274.2$  ppm, Figure 2 right, shows the typical behavior for the presence of a paramagnetic atom in the Wells-Dawson structure;<sup>23</sup> the up-field peak can be assigned to the phosphorus atom distal to  $\text{Co}^{\text{II}}$  and down-field peak can be assigned to the phosphorus atom vicinal to  $\text{Co}^{\text{II}}$ . The two peaks at  $-14.1$  and  $-7.4$  ppm that appeared upon ozonation are associated with the formation of  $[(\text{POMCo})_2\text{O}]$  as will be detailed below. After 30 min at 10 mM  $\text{K}[\text{POMCo}^{\text{II}}\text{H}_2\text{O}]$  a conversion of 80-85% was measured. The appearance of small minor ( $\sim 5\%$ ) set of peaks at  $-8.1$  and  $-13.8$  ppm was also observed. These peaks are assigned to a one electron oxidized species  $[\text{POMCo}^{\text{III}}\text{H}_2\text{O}]$  since treatment of  $\text{K}[\text{POMCo}^{\text{II}}\text{H}_2\text{O}]$  with a one-electron oxidant such as  $\text{K}_2\text{S}_2\text{O}_8$  yielded a spectrum with peaks at these chemical shifts, Figure S1. It is notable that after purging the ozonated solution with an inert gas within 1 h at room temperature, only the major peaks in the  $^{31}\text{P}$  NMR spectrum associated with  $[(\text{POMCo})_2\text{O}]$  disap-

pear with the reappearance of the peaks of the original  $[\text{POMCo}^{\text{II}}\text{H}_2\text{O}]$  species.  $[\text{POMCo}^{\text{III}}\text{H}_2\text{O}]$  was not formed during this reverse reaction.  $[\text{POMCo}^{\text{III}}\text{H}_2\text{O}]$  was constant as a minor impurity and remained unchanged in the solution; it was stable for more than a week. There is no disproportionation of  $[\text{POMCo}^{\text{II}}\text{H}_2\text{O}]$  and  $[(\text{POMCo})_2\text{O}]$  to  $[\text{POMCo}^{\text{II}}\text{H}_2\text{O}]$ .

The optical absorption spectrum of the ozonated and then Ar purged solution of  $\text{K}[\text{POMCo}^{\text{II}}\text{H}_2\text{O}]$  is presented in Figure 3. At  $150\ \mu\text{M}$  one can easily see new absorption peaks at  $\lambda_3 = 381\ \text{nm}$ ,  $\lambda_4 = 507\ \text{nm}$ . At lower concentration of  $12\ \mu\text{M}$  the peaks in the UV region attributable to the ozonated species cannot be deconvoluted because of the strong charge transfer peak of the polyoxometalate framework. However, a difference spectrum clearly revealed two additional peaks at  $\lambda_1 = 262\ \text{nm}$ ,  $\lambda_2 = 304\ \text{nm}$ . Notably,  $[\text{POMCo}^{\text{III}}\text{H}_2\text{O}]$  has a very different UV-vis spectrum from that of  $[(\text{POMCo})_2\text{O}]$ , Figure S2.

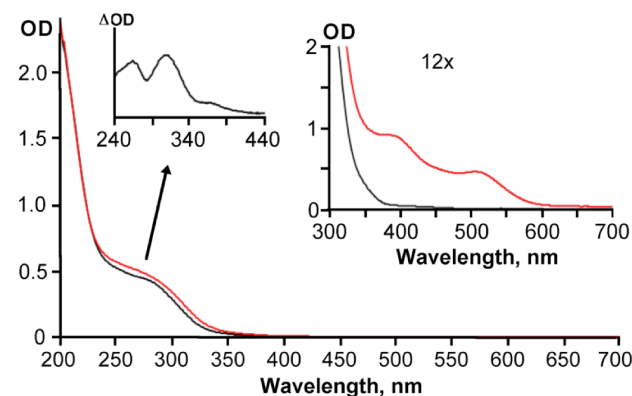


Figure 3. The UV-vis spectra of  $12\ \mu\text{M}$  and  $150\ \mu\text{M}$  (right insert) of aqueous solutions of  $\text{K}[\text{POMCo}^{\text{II}}\text{H}_2\text{O}]$  at 22 °C (black line) and of an ozonated solution (red line) along with the difference spectrum for the UV - range.

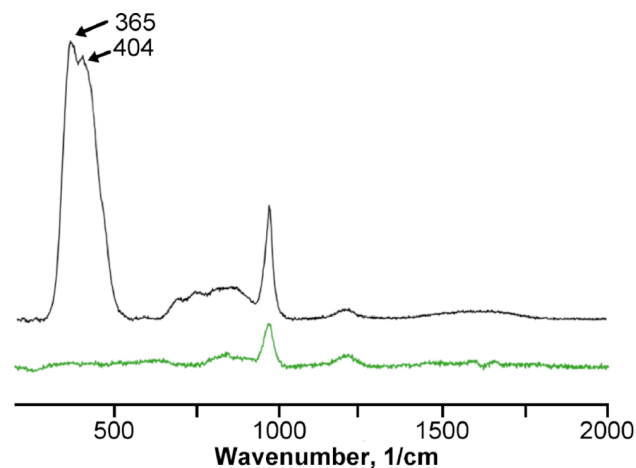


Figure 4. The Raman spectrum of 10 mM aqueous solutions of  $\text{K}[\text{POMCo}^{\text{II}}\text{H}_2\text{O}]$  before (green) and after (black) ozonolysis.

Additional structural data on the ozonated species was obtained by Raman spectroscopy, Figure 4. The most notable feature is the appearance of the strong peaks at  $365$  and  $404\ \text{cm}^{-1}$ . These peaks can very reasonably be assigned to the symmetric  $\text{Co}-\text{O}-\text{Co}$  bond stretching vibrations, expected to be intense and in this very energy region due to the linearity of the bridging oxo ligand.<sup>24</sup> The asymmetric  $\text{Co}-\text{O}-\text{Co}$  bond

stretching vibrations are expected at 800-900  $\text{cm}^{-1}$ , but are weak.<sup>24</sup> Furthermore, for a linear Co–O–Co bond, no or only a small isotope effect is expected.<sup>24</sup> Indeed, the Raman spectra is essentially unchanged when  $[(\text{POMCo})_2\text{O}]$  was prepared in  $\text{H}_2^{18}\text{O}$ , though as will be shown below in the reactivity experiments, preparation of  $[(\text{POMCo})_2\text{O}]$  in  $\text{H}_2^{18}\text{O}$  leads to an O-18 labeled compound. Importantly, these vibrations can be observed both in the solid state Raman and IR, Figure S3, indicating that the same species are present in the solid state as well as in aqueous solution. Finally and also notable is the observation that the Raman spectrum of  $\text{K}[(\text{POMCo}^{\text{III}}\text{H}_2\text{O})]$  is indistinguishable from that of  $\text{K}[(\text{POMCo}^{\text{III}}\text{H}_2\text{O})]$ .

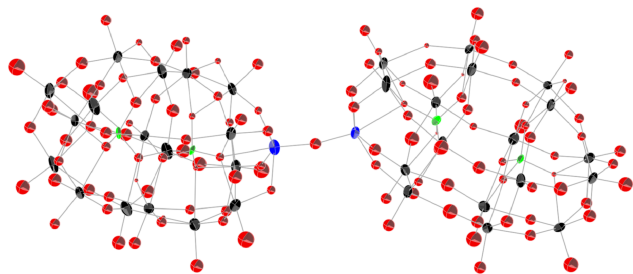


Figure 5. ORTEP structure (with 50% probability ellipsoids) of  $[(\text{POMCo})_2\text{O}]$ . Solvent molecules and cations are not shown for clarity. P – green; W – black; O – red; Co – blue. Note – the Co occupancies are 90% and 77%, the remainder refined as W.

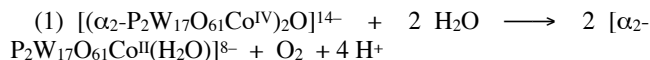
After numerous attempts over a period of two years, we were finally able to crystallize the product of the ozonation reaction, by addition of tetramethyl ammonium fluoride at  $\sim 0^\circ\text{C}$ , followed by precipitation and re-crystallization from a warm aqueous solution. Note that other available tetramethyl ammonium halides ( $\text{Cl}^-$ ,  $\text{Br}^-$ ) reacted immediately with the oxidized species. The compound is unstable under these conditions, *vide infra* and the solution initially contains about 25-30%  $[(\text{POMCo}^{\text{III}}\text{H}_2\text{O})]$  as measured by  $^{31}\text{P}$  NMR. The crystallization needs to occur within 10-15 minutes before too much decay of  $[(\text{POMCo})_2\text{O}]$  occurred and only *very small*, 150 by 10 by 10 micron, needle-like crystals were formed. Despite this limitation and some disorder, the crystal structure as determined by single crystal X-ray diffraction clearly indicates the formation of a Co-O-Co dimer species between two Wells-Dawson anions, Figure 5. Three diffraction measurements were made on different batches of crystals and all showed this result. From the crystal structure Co-O<sub>bridge</sub> bond lengths of 1.79(3) and 1.77 (4) Å and Co-O<sub>bridge</sub>-Co bond angle of 167(2) $^\circ$  was determined. One may note that the best solution to the X-ray diffraction data indicates a partial occupancy of the Co atoms (90% and 77%). One explanation is that there are also Co-O-W bridged species. However, in such a situation, one would expect to observe an indicative spectroscopic feature in the solution  $^{31}\text{P}$  NMR. Another more likely explanation is that  $[(\text{POMCo})_2\text{O}]$  compound co-crystallizes with  $[(\text{POMCo}^{\text{III}}\text{H}_2\text{O})]$ , present as an impurity. Indeed, the MAS  $^{31}\text{P}$  NMR spectrum of crystalline  $[(\text{POMCo})_2\text{O}]$ , Figure S4, shows the presence of the  $[(\text{POMCo}^{\text{III}}\text{H}_2\text{O})]$  as an impurity. Since,  $[(\text{POMCo}^{\text{III}}\text{H}_2\text{O})]$ , does not crystallize anisotropically, there is likely some disorder at all positions; it more observable at the unique cobalt positions since some W at a Co position has a much larger effect than some Co at a W position. The counteranions in the structure ( $\text{Me}_4\text{N}^+$  and  $\text{K}^+$ ) are partially disordered and could not be well refined.

Direct measurement of the oxidation state of the cobalt atom proved to be impossible. X-ray photon spectroscopy (XPS)

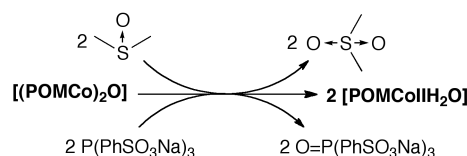
measurements, Figure S5, carried out on  $[(\text{POMCo}^{\text{III}}\text{H}_2\text{O})]$ ,  $[(\text{POMCo}^{\text{III}}\text{H}_2\text{O})]$  and  $[(\text{POMCo})_2\text{O}]$  clearly showed a higher binding energy for  $\text{Co}^{\text{III}}$  versus  $\text{Co}^{\text{II}}$  as would be expected, however the reducing conditions of the XPS measurements, as was also visible by eye, reverted  $[(\text{POMCo})_2\text{O}]$  back to a  $\text{Co}^{\text{II}}$  species. Attempts to use electron energy loss spectroscopy (EELS),<sup>20</sup> Figure S6, also failed because of an insufficient signal to noise ratio for an analytical analysis. Magnetic susceptibility measurements, Figure S7, however, showed that  $[(\text{POMCo}^{\text{III}}\text{H}_2\text{O})]$  is paramagnetic and  $[(\text{POMCo}^{\text{III}}\text{H}_2\text{O})]$  is diamagnetic while  $[(\text{POMCo})_2\text{O}]$  showed a *significant* decrease in the magnetic susceptibility of one order of magnitude and showed anti-ferromagnetic behavior. The low magnetic susceptibility may explain the chemical shifts and narrow lines observed in the  $^{31}\text{P}$  NMR spectrum.  $[(\text{POMCo})_2\text{O}]$  is EPR silent as expected for an antiferromagnetically coupled compound although some impurity of  $[(\text{POMCo}^{\text{III}}\text{H}_2\text{O})]$  can be observed in the solid sample but not in solution.

### Reactivity Studies

Since  $[(\text{POMCo})_2\text{O}]$  is not stable in water and reverts back to  $[(\text{POMCo}^{\text{III}}\text{H}_2\text{O})]$  as identified by  $^{31}\text{P}$  NMR *but not to*  $[(\text{POMCo}^{\text{III}}\text{H}_2\text{O})]$ , it was reasonable to assume that water is oxidized to  $\text{O}_2$ . Indeed, we were able to measure by gas burette and analysis by gas chromatography the formation of one equivalent of  $\text{O}_2$  per equivalent of  $[(\text{POMCo})_2\text{O}]$ , Equation 1. This reaction stoichiometry also points toward the formulation of  $[(\text{POMCo})_2\text{O}]$  as *formally* a bis- $\text{Co}^{\text{IV}}$  compound since the formation of  $\text{O}_2$  is necessarily a four-electron oxidation. See below for the more exact electronic structure analysis. A reaction where  $[(\text{POMCo})_2\text{O}]$  was prepared in  $\text{H}_2^{18}\text{O}$  yielded  $^{18}\text{O}_2$  only. The cycle of formation of  $[(\text{POMCo})_2\text{O}]$  from 10 mM  $[(\text{POMCo}^{\text{III}}\text{H}_2\text{O})]$  and oxidation of water was repeated 10 times without any change in yield or rate of formation of  $\text{O}_2$ .



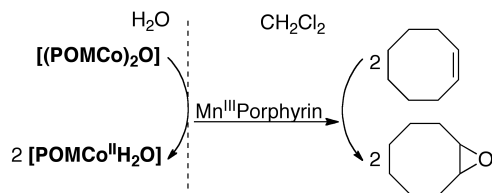
A kinetic study of the water oxidation reaction *in dilute solutions* by the method of initial rates, Figure S8, carried out by measuring the optical density at 507 nm, the peak in the visible spectrum associated with  $[(\text{POMCo})_2\text{O}]$  (Figure 2), reveals that the reaction is indeed first order in  $[(\text{POMCo})_2\text{O}]$ . A first order rate constant,  $k_{\text{obs}} = 5.04 \times 10^{-5} \text{ s}^{-1}$  at  $22^\circ\text{C}$  was calculated. Further study of the rate as a function of temperature, Figure S9, yielded measured activation energies,  $\Delta H^\ddagger_{298} = 8.7 \text{ kcal/mol}$ ,  $\Delta S^\ddagger_{298} = -48.6 \text{ cal/mol K}$  and  $\Delta G^\ddagger_{298} = 23.2 \text{ kcal/mol}$ . Reactions in  $\text{D}_2\text{O}$  showed no kinetic isotope effect.



**Scheme 1.** Oxidation of water-soluble nucleophiles by  $[(\text{POMCo})_2\text{O}]$ .

The reactivity of  $[(\text{POMCo})_2\text{O}]$  was also assessed towards nucleophilic water-soluble organic compounds in oxygen transfer reactions. Thus, sulfonated triphenylphosphine,  $\text{P}(\text{PhSO}_3\text{Na}^+)_3$  was quantitatively oxidized within seconds to the corresponding phosphine oxide,  $\text{P}(\text{O})(\text{PhSO}_3\text{Na}^+)_3$  in  $\text{P}(\text{PhSO}_3\text{Na}^+)_3/[(\text{POMCo})_2\text{O}]$  of 2 to 1, Scheme 1. Similarly dimethyl sulfoxide was quantitatively oxidized to the corresponding sulfone, Scheme 1.

Interestingly, epoxidation of alkenes was not observed in a necessarily biphasic reaction, however in the presence of a slight excess of  $\text{Mn}^{\text{III}}$ tetramesityl porphyrin as an oxygen atom acceptor to form a competent epoxidizing intermediate, cyclooctene was oxidized within a few minutes to yield two equivalents of cyclooctene oxide per equivalent  $[(\text{POMCo})_2\text{O}]$ , Scheme 2.  $\text{Mn}^{\text{III}}$ tetramesityl porphyrin does not catalyze the epoxidation of cyclooctene with  $\text{O}_2$ ;  $\text{O}_2$  is not an intermediate in this reaction. When  $[(\text{POMCo})_2\text{O}]$  was prepared in  $\text{H}_2^{18}\text{O}$  only 18-O labeled cyclooctene oxide was formed. All the aforementioned stoichiometric reactions support the conclusion that  $[(\text{POMCo})_2\text{O}]$  is a four electron oxidant.



**Scheme 2.** Biphasic epoxidation of alkenes in the presence of  $\text{Mn}^{\text{III}}$ (tetramesityl)porphyrin.

**Table 1.** Oxidation of alcohols by  $[(\text{POMCo})_2\text{O}]$

Substrate	Product	Yield, mol%	BDE, mol <sup>27</sup>	kJ/
but-3-en-2-ol	but-3-en-2-one	65	Unknown <sup>a</sup>	
prop-2-en-1-ol	acrolein	52	341.1±7.5	
2-propanol	acetone	20	380.7±4.2	
ethanol	acetaldehyde	2	396.6±4.2	

A solution of 5 mM  $\text{K}[(\text{POMCo})_2\text{O}]$  and 40 mM substrate in  $\text{D}_2\text{O}$  was prepared at 0 °C and let to warm to RT. Products were quantified by  $^1\text{H}$  and  $^{31}\text{P}$  NMR. (a) The BDE of but-3-en-2-ol has not been reported but the radical chlorination of but-3-en-2-ol is faster than that of allyl alcohol.<sup>28</sup>

In reactions of water-soluble allylic alcohols with  $[(\text{POMCo})_2\text{O}]$ , only C–H activation was observed with the chemoselective product formation of ketones or aldehydes. The propensity for C–H bond activation was tested on a series of water-soluble alcohols, Table 1. The general trend is quite clear. Oxidation is a function of the C–H bond dissociation energy (BDE), which is a strong indication that the oxidation proceeds either by a hydrogen atom transfer (HAT) mechanism or via formation of a metal alkoxide followed by rate determining  $\beta$ -hydrogen elimination.<sup>25</sup> It should be noted that the chemical yields, especially for simple aliphatic alcohols is low, likely due to competing water oxidation. This is most likely just a concentration effect since the concentration of water is ~55 M versus only 40 mM alcohol. In fact,  $[(\text{POMCo})_2\text{O}]$  is quite a potent oxidant, capable even of catalytic, but not stoichiometric oxidation of very difficult to oxidize fluoro-substituted alcohols such as trifluoroethanol that has an *ab initio* calculated C–H BDE of 418 kJ/mol.<sup>26</sup> Thus, a solution of 5 mM  $\text{K}[(\text{POMCo})_2\text{O}]$  and 50 mM hexafluoroisopropanol in  $\text{H}_2\text{O}$  under a flow of ozone at ~0 °C, yielded 36 mol% hexafluoroacetone by  $^{19}\text{F}$  NMR after 30 min.

The direct measurement of the reaction rates of the oxidation of methanol and ethanol in 10 vol% solutions in water is shown in Figure 6. Note that the reaction conditions are quite different than those described above in Table 1. The disappearance of  $[(\text{POMCo})_2\text{O}]$  species is faster in presence of ethanol than methanol as would be expected for the lower BDE of the reactive C–H bond in ethanol versus methanol. Both alcohols were oxidized much faster than water. Furthermore, a kinetic isotope effect for the oxidation of methanol was measured and yielded a  $k_{\text{H}}/k_{\text{D}} = 5.65 \pm 0.2$ . Both these kinetics measurements support a HAT or an alkoxide/ $\beta$ -hydrogen elimination mechanism.

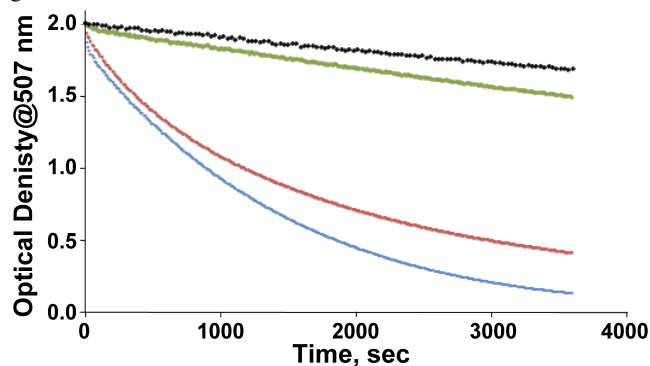


**Figure 6.** Kinetic profiles of the decay of a 0.15 mM aqueous  $[(\text{POMCo})_2\text{O}]$  at 22 °C. black- $\text{H}_2\text{O}$  only; blue-10 vol% (1.71 M) ethanol; red-10 vol% (2.47 M) methanol; green-10 vol% (2.46 M) methanol- $\text{d}_4$ .  $k_{\text{obs}} = 4.41 \times 10^{-4}$  1/s (MeOH);  $k_{\text{obs}} = 7.81 \times 10^{-5}$  1/s (MeOH- $\text{d}_4$ );  $k_{\text{obs}} = 5.04 \times 10^{-4}$  1/s (EtOH).

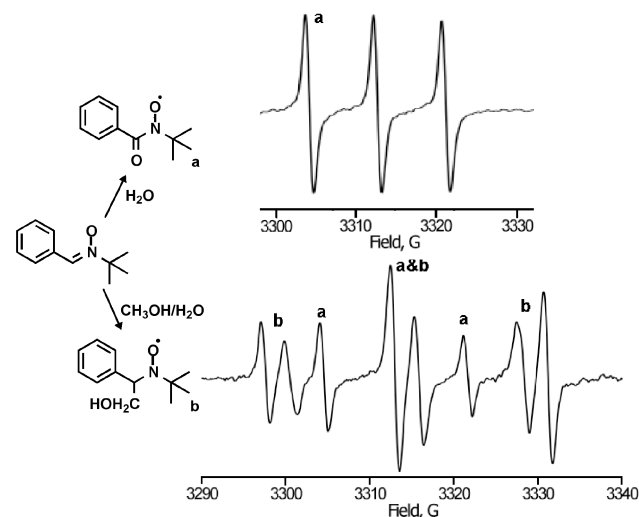


**Figure 7.** EPR spectra of spin adducts generated at 293 K from 5 mM  $\text{K}[(\text{POMCo})_2\text{O}]$  and 50 mM PBN in water (top) and in 5.5 vol%  $\text{CH}_3\text{OH}/\text{H}_2\text{O}$  mixture (bottom).

Further support for the oxidation of alcohols by a HAT as opposed to an alkoxide/ $\beta$ -hydrogen elimination mechanism was obtained by reacting  $\text{K}[(\text{POMCo})_2\text{O}]$  with a spin trap, *N*-tert-butyl- $\alpha$ -phenyl-nitrone (PBN), Figure 7. In water only, a triplet spectrum ( $A_{\text{N}} = 8.5$  G) was obtained. From the literature and based on the hyperfine coupling constants and computer simulation the spin-adduct product was identified as **PBNOx**.<sup>29</sup> On the other hand the same experiment in 5.5 vol%  $\text{CH}_3\text{OH}/\text{H}_2\text{O}$  solution both the **PBNOx** and a new species (with a hexet spectrum ( $A_{\text{N}} = 15.1$  G,  $A_{\text{H}} = 3.1$  G) was observed. This spectrum is typical of spin adducts of PBN with  $\text{HOCH}_2\bullet$ ,

CH<sub>3</sub>O•, or HO• radicals, which are difficult to differentiate.<sup>29</sup> However, reaction in 5.5 vol% CD<sub>3</sub>OH/H<sub>2</sub>O showed almost exclusive formation of **PBNOx** leading to the conclusion that the sextet observed in the EPR can be associated with the spin-adduct of **PBN** with HOCH<sub>2</sub>• because of the higher BDE and thus less radical formation in CD<sub>3</sub>OH versus that in CH<sub>3</sub>OH.

#### Computational Analysis of the Electronic Structure

Computational methods have been extensively used to analyze the structure, electronic properties and reactivity of polyoxometalates.<sup>30</sup> To characterize the electronic structure of the observed [(**POMCo**)<sub>2</sub>O] anion, DFT calculations using the B3LYP functional were performed on experimentally prepared Wells-Dawson dimer with cobalt atoms in formal oxidation states III and IV, [(P<sub>2</sub>W<sub>17</sub>O<sub>61</sub>Co<sup>III</sup>)<sub>2</sub>O]<sup>16-</sup> and [(P<sub>2</sub>W<sub>17</sub>O<sub>61</sub>Co<sup>IV</sup>)<sub>2</sub>O]<sup>14-</sup>. Full optimization was performed using the PCM approach to model the water solvent. The two polyoxometalate frameworks were arranged in a *trans* disposition to retain a symmetry plane. For [(P<sub>2</sub>W<sub>17</sub>O<sub>61</sub>Co<sup>III</sup>)<sub>2</sub>O]<sup>16-</sup>, where there is no experimental analogue the ground state is a singlet as expected for a Co(III) in an octahedral environment. Importantly, the frontier orbitals display an electronic structure where the two highest occupied orbitals (HOMO and HOMO-1) are mainly localized on the Co-O-Co bridging unit and have a significant contribution of p orbitals from the bridging oxygen and only a minor contribution of cobalt d-orbitals, Figure 8. The LUMO is centred on the polyoxometalate framework. This result is in line with the common axiom that it is difficult for cobalt ions to lose their fourth electron.

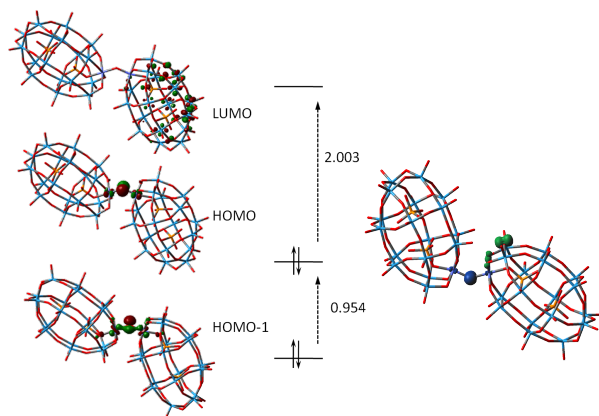


Figure 8. Molecular orbital diagram and spin density distributions. Left - orbital representations of the LUMO, HOMO and HOMO-1 for the theoretical species, [(P<sub>2</sub>W<sub>17</sub>O<sub>61</sub>Co<sup>III</sup>)<sub>2</sub>O]<sup>16-</sup> with energy gaps in eV. Right - computed (α-β) spin density representation for the [(α<sub>2</sub>-P<sub>2</sub>W<sub>17</sub>O<sub>61</sub>Co<sup>IV</sup>)<sub>2</sub>O]<sup>14-</sup>, [(**POMCo**)<sub>2</sub>O], species in the Ms=0 broken symmetry state.

The calculation for [(P<sub>2</sub>W<sub>17</sub>O<sub>61</sub>Co<sup>IV</sup>)<sub>2</sub>O]<sup>14-</sup> or [(**POMCo**)<sub>2</sub>O] shows a reasonable fit of the Co-O<sub>bridge</sub> bond lengths (1.806 and 1.784 Å) compared to the experimental values of 1.79 and 1.77 Å. The calculated Co-O<sub>bridge</sub>-Co angle is, however, more acute, 139.1 deg versus the experimental values of 167 deg.<sup>31</sup> The first oxidation of [(P<sub>2</sub>W<sub>17</sub>O<sub>61</sub>Co<sup>III</sup>)<sub>2</sub>O]<sup>16-</sup> occurs on the bridging Co-O-Co oxygen as a consequence of the finding that the HOMO and HOMO-1 are mainly localized on the Co-O-Co bridging unit. The second electron, however, can not be removed from the same oxygen atom and therefore the electron spin density computed for two-electron oxidizing [(P<sub>2</sub>W<sub>17</sub>O<sub>61</sub>Co<sub>2</sub>O)]<sup>14-</sup> in the Ms=0 broken symmetry state shows the formation of cation radicals (holes) with one unpaired electron localized on

the bridging oxygen and the other one localized on an oxygen atom in the polyoxometalate framework. A similar finding was also reported in another theoretical analysis where the description of an oxidized cobalt-oxo reactive species was described as a Co<sup>III</sup>O• radical and not Co<sup>IV</sup>O.<sup>32</sup> The singlet-triplet separation has been estimated to be about 30 cm<sup>-1</sup> showing a weak antiferromagnetic coupling of the unpaired electrons. Figure S11 shows the spin density computed for the triplet state.

Calculations based on a smaller Lindqvist type polyoxometalate, [(W<sub>5</sub>O<sub>18</sub>Co)<sub>2</sub>O]<sup>9-</sup>, allows computations without symmetry restrictions. Overall, no significant differences were observed in the geometric and electronic structure of the Lindqvist derivative in comparison to the Wells-Dawson one, Figure S12. The fluxionality of the Co-O-Co bond and the bond angle in the dimer was also tested in order to evaluate if a change in the geometric structure could modify the electronic structure of [(**POMCo**)<sub>2</sub>O]. A displacement of 0.5 Å of the bridging oxygen from its almost symmetrical optimal position towards one of the cobalt centres increases the energy by only 0.4 kcal·mol<sup>-1</sup>. Another displacement of 0.5 Å leads to a structure with the bridging oxygen forming two asymmetric bonds with bond distances of 1.750 Å and 1.866 Å, a structure that is 1.7 kcal·mol<sup>-1</sup> above the optimal structure. The shortening of the bond does not modify, however, the Co<sup>III</sup>O• radical nature of the bond. The potential influence of the Co-O-Co bond angle on the electronic structure of the dimer was also tested. When the Co-O-Co bond angle is changed from 170° to 130° the energy changes only by 4 kcal·mol<sup>-1</sup> and there is no significant effect on the electronic structure of the anion. To test for the fidelity of the computations, calculations were also carried out using the PBE0 functional, especially because it was reported that using the PBE0 functional the electronic structure of the cubane cluster [Co<sub>4</sub>O<sub>4</sub>(C<sub>5</sub>H<sub>5</sub>N)<sub>4</sub>(CH<sub>3</sub>CO<sub>2</sub>)<sub>4</sub>]<sup>+</sup> can be described as a Co<sup>IV</sup>Co<sup>III</sup><sub>3</sub>O<sub>4</sub> species where the electron spin density is spread almost equally over the eight core atoms.<sup>15c</sup> In our dimer system, however, the spin density remains qualitatively unaltered using the PBE0 functional, Figure S13. Finally, we have carried out CASSCF calculations on the complete Lindqvist dimer anion using the geometry optimized at the DFT level. Multiconfigurational wave functions were constructed by distributing 14 electrons over 12 orbitals. The lowest root has precisely the same character as observed in the DFT calculations; one hole on the bridging oxygen and another hole localized on one of the oxygens of the Lindqvist cage, Figure S14. Among the twelve lowest CASSCF roots, there are no electronic states with extra holes on the Co ions.

#### CONCLUSIONS

A high valent species based on a cobalt-substituted Wells-Dawson polyoxometalate, [(**POMCo**)<sub>2</sub>O], has been isolated by oxidation of a known [**POMCo**<sup>III</sup>H<sub>2</sub>O] compound with ozone. The solution of the X-ray diffraction measurements reveals an almost linear, 169.4(14)°, dicobalt-μ-oxo unit with an average Co-O bond length of 1.81 Å. The electronic structure as determined by DFT and CASSCF calculations indicates that [(**POMCo**)<sub>2</sub>O] is best represented as a compound with two cobalt (III) atoms and two oxygen cation radicals (O•) one at the bridging oxygen atom and the other in the polyoxometalate framework. The representation of [(**POMCo**)<sub>2</sub>O] as a bis cobalt (IV) compound seems much less likely.

Solution phase <sup>31</sup>P NMR, UV-vis and Raman spectroscopic studies of [(**POMCo**)<sub>2</sub>O] clearly differentiate [(**POMCo**)<sub>2</sub>O] from the [**POMCo**<sup>III</sup>H<sub>2</sub>O] starting compound and the one electron oxidized analogue [**POMCo**<sup>III</sup>H<sub>2</sub>O] prepared by oxida-

tion with  $K_2S_2O_8$ .  $[POMCo^{III}H_2O]$  is stable in water and did not react with water or other substrates such as alcohols, phosphines or sulfoxide. On the other hand reactions of  $[(POMCo)_2O]$  with  $H_2O$ ,  $P(PhSO_3Na)_3$ ,  $CH_3S(O)CH_3$  and cyclooctene in the presence of a Mn(III)mesitylporphyrin, yielded  $O_2$ ,  $P(O)(PhSO_3Na)_3$ ,  $CH_3S(O)_2CH_3$  and cyclooctene oxide, respectively with co-formation of  $[POMCo^{III}H_2O]$ , but not  $[POMCo^{III}H_2O]$ . The reaction stoichiometries in all these cases show that  $[(POMCo)_2O]$  is a four electron oxidant. Use of  $H_2^{18}O$  as solvent leads to the formation almost exclusively of  $^{18}O_2$  and 18-O labelled oxygenates. The isotope labelling experiments indicate that oxygen atoms in  $[(POMCo)_2O]$ , at least those involved in water oxidation and oxygenation quickly exchange with the solvent.<sup>97</sup> Although  $[(POMCo)_2O]$  does not react directly with alkenes it does activate C-H bonds of alcohols in water where reactivity is a function of the bond dissociation energy. Under catalytic conditions, even more difficult to oxidize fluoro substituted alcohols are oxidized. Reactivity in the alcohol oxidation reactions is proportional to the BDE of the C-H bond that is activated. The rate of oxidation of ethanol was faster than that of methanol and for methanol a kinetic isotope effect of  $5.65 \pm 0.2$  was measured. In addition, EPR spectroscopy in the presence of spin adducts under methanol oxidation conditions shows the intermediacy of a  $\bullet CH_2OH$  radical species. This spin trapping experiments along with the reaction kinetics all point towards a hydrogen atom transfer mechanism for C-H bond activation.

The actual active species involved in the C-H bond activation and oxygen transfer reactions as well as the mechanism of water oxidation to  $O_2$  remains unknown. The observation that the reaction is first order in  $[(POMCo)_2O]$  and that  $[(POMCo)_2O]$  is a four electron oxidant with two equivalents of  $[POMCo^{III}H_2O]$  as products and no observed  $[POMCo^{III}H_2O]$  intermediate suggests an intramolecular mechanism that likely includes addition of a water molecule to the bridge between the cobalt atoms, perhaps to form a bis- $\mu$ -hydroxy complex that rearranges to form  $O_2$ . This intermediate may likely also be involved in C-H bond activation and oxygen transfer reactions. The activation parameters for the water oxidation,  $\Delta H^\ddagger_{298} = 8.7$  kcal/mol,  $\Delta S^\ddagger_{298} = -48.6$  cal/mol K and  $\Delta G^\ddagger_{298} = 23.2$  kcal/mol, indicate a highly ordered transition state. It is notable that for methanol oxidation the activation parameters,  $\Delta H^\ddagger_{298} = 6.9$  kcal/mol,  $\Delta S^\ddagger_{298} = -50.45$  cal/mol K and  $\Delta G^\ddagger_{298} = 21.95$  kcal/mol also indicate a highly ordered transition state for the alcohol oxidation reactions.

## EXPERIMENTAL SECTION

**Polyoxometalate Synthesis.** The cobalt(II) – substituted Wells-Dawson polyoxometalate,  $\alpha_2-K_8P_2Co(H_2O)W_{17}O_{61} \cdot 16H_2O$ ,  $K[POMCo^{III}H_2O]$ , was synthesized according to the published procedure.<sup>34</sup> The cesium,  $Cs[POMCo^{III}H_2O]$ , and tetramethyl ammonium,  $TMA[POMCo^{III}H_2O]$ , salts were prepared by addition to a stirred solution of  $[Co^{III}H_2O]$  in water (0.1 mmol, 10 ml) 8.8 equivalents of  $CsCl$  or  $(CH_3)_4NF$  respectively (0.88 mmol) in a minimum amount of water. The resulting suspension was stirred vigorously for 20 min, filtered and recrystallized from hot water. The oxidized analogues,  $Cs[(POMCo)_2O]$  and  $TMA[(POMCo)_2O]$  were isolated at 0 °C from the ozonated  $K[POMCo^{III}H_2O]$  solution after purging of excess ozone via precipitation by the procedure described just above. The solids were separated by centrifugation, dried and kept under an inert atmosphere at -80 °C. Very small single crystals suitable for X-ray analysis were obtained by precipitation with tetramethyl ammonium fluoride, followed by very fast re-crystallization

from a slightly warmed (~35 °C) aqueous solution. The diffraction data need to be collected as fast as possible after crystallization.

**Table 2. Crystal data and structure refinement for  $[(POMCo)_2O]$ .**<sup>35</sup>

	$[(POMCo)_2O]$
Empirical formula	$2(Co_{1.67}O_{123}P_4W_{34.33}), 19(C_4H_{12}N), 11(O)$
Formula weight	9294.56
Crystal system	monoclinic
Space group	P2(1)/c
a, Å	27.517(6)
b, Å	29.404(6)
c, Å	26.160(8)
$\alpha$ , deg	90.00
$\beta$ , deg	112.306(9)
$\gamma$ , deg	90.00
V (Å <sup>3</sup> )	19583(8)
Z	4
$d_{calc}$ (mg/cm <sup>3</sup> )	3.153
$\mu$ (mm <sup>-1</sup> )	20.326
Reflections	86029
Unique Reflections	28011
$R_{int}$	0.1490
R [ $I > 2\sigma(I)$ ]	$R_1 = 0.0822$ $wR_2 = 0.1725$
Goodness of Fit	0.914

$$R_1 = \sum ||F_o| - |F_c|| / \sum |F_o|; \quad wR_2 = \{ \sum [w(F_o^2 - F_c^2)^2] / \sum w(F_o^2)^2 \}^{1/2}$$

**X-ray Structure Determination.** Crystals were placed in Paratone oil (Hampton research) and mounted on a MiTeGen cryoloop before being flash cooled in liquid nitrogen. Crystal data for compound  $[(POMCo)_2O]$  were collected at 100 K using a Bruker Kappa ApexII CCD diffractometer with Mo-K $\alpha$  ( $\lambda = 0.71073$  Å) radiation, graphite monochromator, and Miracol optics. The data were integrated with Bruker Apex2 Saint Software. Routine Lorentz and polarization corrections were applied and multi-scan absorption corrections were performed using SADABS. Direct methods were performed using the program SHELXS-97. The tungsten and cobalt atoms were successfully located in the structure solution and subsequent cycles of refinement using SHELXL-97 located the remaining atoms including tertiary methyl ammonium counter-ions. The refinements were weighted full-matrix least-squares against  $|F^2|$  using all data. In the final stages of refinement SQUEEZE was used due to the large voids and remaining disordered counter-ions and solvent molecules. In the refinement W and Co atoms were refined anisotropically and oxygen, and carbon atoms were refined isotropically. Hydrogen atoms were placed

in calculated positions and refined in riding mode. Crystal data collection and refinement parameters are given in Table 2 and the complete data can be found in the cif file as supporting information.

**Oxidation of Organic Substrates.** Oxidation reactions were typically carried out in 1 mL 10 mM D<sub>2</sub>O solutions of **K[POMCo<sup>III</sup>H<sub>2</sub>O]**, which was ozonated for 30 min at 0 °C, and purged with argon. The amount of **K[(POMCo)<sub>2</sub>O]** was quantified by <sup>31</sup>P NMR and then 4 equivalents of a substrate were added. The solution was left to heat up slowly to room temperature with stirring. Products were identified and quantified by <sup>1</sup>H NMR using TMS as external standard. Mn<sup>III</sup>(TMP)Cl was prepared metallation of tetramesitylporphyrin. A solution of Mn<sup>III</sup>(TMP)Cl (10 μmol) and cis-cyclooctene (50 μmol) in 1 mL dichloromethane was added to a 5 μmol **[(POMCo)<sub>2</sub>O]** in 1 mL water. The amount of cyclooctene oxide was determined by GC measurements using decane as external standard. 18-O labelled products were identified by GC-MS.

**Oxidation of Water.** The volume of O<sub>2</sub> was measured by direct methods, via connecting of the reaction vessel with a U-tube to a calibrated micro burette with collection of the gas released. Three mL of a 12 mM **K[POMCo<sup>III</sup>H<sub>2</sub>O]** solution was treated with ozone (concentration - 25 mg/L, rate - 6.25 mg/min) for 30 min and then purged/degassed with Ar to yield a 5 mM solution (by <sup>31</sup>P NMR) of **K[(POMCo)<sub>2</sub>O]**. From this solution that contains 15 μmol **K[(POMCo)<sub>2</sub>O]** was released 0.33 ml O<sub>2</sub> (13.5 μmol) at 20 °C (average over three experiments). The solubility of O<sub>2</sub> at 20 °C is 7.6 μg/mL so 3 mL water can optimally contain an additional 0.7 μmol O<sub>2</sub>. The O<sub>2</sub> yield can be estimated to be 95%.

**Computational Details.** All reported calculations were performed with the Gaussian09 package at DFT level by means of the hybrid exchange-correlation B3LYP functional.<sup>36</sup> For P, Co and W atoms, the LANL2DZ pseudopotential was used.<sup>37</sup> The 6-31g(d,p) basis set was used for O atoms directly bound to Co and the 6-31g basis set for the rest of atoms.<sup>38</sup> All the structures were optimized in water solution using IEF-PCM approach to model the solvent effects (ε = 78.36 and UFF radii).<sup>39</sup> Open shells were computed at unrestricted DFT level. The Ms=0 broken symmetry state for the 2e-oxidized species was determined using the broken symmetry approach at the geometry computed for triplet state. For the sake of comparison spin density distributions were also determined with the hybrid PBE0 (Perdew–Burke–Ernzerhof exchange-correlation) functional.<sup>40</sup> CASSCF calculations were performed using MOLCAS<sup>41</sup> and with the same basis set as in the DFT calculations.

## ASSOCIATED CONTENT

**Supporting Information.** More details on experimental and computational methods and additional, spectroscopic, kinetic and computational data. This material is available free of charge via the Internet at <http://pubs.acs.org>.

## AUTHOR INFORMATION

### Corresponding Author

\* Ronny.Neumann@weizmann.ac.il

## ACKNOWLEDGMENT

This research was supported by the Israel Science Foundation grant # 1073/10, the Helen and Martin Kimmel Center for Molecular Design, the Spanish Ministry of Science and Innovation

(Project No. CTQ2011-29054-C02-01) and by the Generalitat de Catalunya (2009SGR462 and XRQTC). Gregory Lars Olsen is thanked for the MAS <sup>31</sup>P NMR measurements. RN is the Rebecca and Israel Sieff Professor of Chemistry.

## REFERENCES

- Torres Pazmino, D. E.; Winkler, M.; Glieder, A.; Fraaije, M. W. *J. Biotech.* **2010**, *146*, 9-24.
- Messinger, J.; Noguchi, T.; Yano, J. *RSC Energy Environ. Ser.* **2012**, *5*, 163-207.
- Navarro, R. M.; Pena, M. A.; Fierro, J. L. G.; *Chem. Ind.* **2006**, *108*, 463-490.
- Nocera, D. G. *Acc. Chem. Res.* **2012**, *45*, 767-776.
- Que, L., Jr; Tolman, W. B. *Nature* **2008**, *455*, 333-340.
- (a) Liu, X.; Wang, F. *Coord. Chem. Rev.* **2012**, *256*, 1115-1136. (b) Du, P.; Eisenberg, R. *Energy Environ. Sci.* **2012**, *5*, 6012-6021. (c) McAlpin, J. G.; Stich, T. A.; Casey, W. H.; Britt, R. D. *Coord. Chem. Rev.* **2012**, *256*, 2445-2452. (d) Jiao, F.; Frei, H. *Energy Environ. Sci.* **2010**, *3*, 1018-1027.
- (a) Sheldon, R. A.; Kochi, J. K. *Metal-Catalyzed Oxidations of Organic Compounds*, Academic, New York, 1981. (b) Oxygen Complexes and Oxygen Activation by Transition Metals Martell, A. E. Sawyer, D. T. eds., Plenum, New York, 1988; (c) Dioxygen Activation and Homogeneous Catalytic Oxidation, *Stud. Surf. Sci. Catal.* **1991**, *66*, 1-696.
- (a) Koola, J. D.; Kochi, J. K. *J. Org. Chem.* **1987**, *52*, 4545-4553. (b) X. Zhang, K. Sasaki, C. L. Hill, *J. Am. Chem. Soc.*, **1996**, *118*, 4809-4816.
- (a) Egan, Jr., J. W.; Haggerty, B. S.; Rheingold, A. L.; Sendlinger, S. C.; Theopold, K. H. *J. Am. Chem. Soc.* **1990**, *112*, 2445-2446. (b) Nam, I. Kim, W.; Kim, Y.; Kim, C. *Chem. Commun.* **2001**, 1262-1263. (c) Song, Y. J.; Hyun, M. Y.; Lee, J. H.; Lee, H. G.; Kim, J. H.; Jang, S. P.; Noh, J. Y.; Kim, Y.; Kim, S.-J.; Lee, S. J.; Kim, C. *Chem. Eur. J.* **2012**, *18*, 6094-6101.
- Pfaff, F. F.; Kundu, S.; Risch, M.; Pandian, S.; Heims, F.; Pryjomska-Ray, I.; Haack, P.; Metzinger, R.; Bill, E.; Dau, H.; Comba, P.; Ray, K. *Angew. Chem. Int. Ed.* **2011**, *50*, 1711-1715.
- Lacy, D. C.; Park, Y. J.; Ziller, J. W.; Yano, J.; Borovik, A. S. *J. Am. Chem. Soc.* **2012**, *134*, 17526-17535.
- (a) Brunschwig, B. S.; Chou, M. H.; Creutz, C.; Ghosh, P.; Sutin, N. *J. Am. Chem. Soc.* **1983**, *105*, 4832-4833. (b) Shafirovich, V. Ya.; Khannanov, N. K.; Strelets, V. V. *Nouv. J. Chim.* **1980**, *4*, 81-84.
- (a) Kanan, M. W.; Nocera, D. G. *Science* **2008**, *321*, 1072-1075. (b) Pijpers, J. J. H.; Winkler, M. T.; Surendranath, Y.; Buonassisi, T.; Nocera, D. G. *Proc. Natl. Acad. Sci. USA* **2011**, *108*, 10056-10061. (c) Surendranath Y.; Lutterman D. A.; Liu Y.; Nocera D. G. *J. Am. Chem. Soc.* **2012**, *134*, 6326-6336. (d) Symes M. D.; Surendranath Y.; Lutterman D. A.; Nocera, D. G. *J. Am. Chem. Soc.* **2011**, *133*, 5174-5177. (e) Kanan, M. W.; Yano, J.; Surendranath, Y.; Dinca, M.; Yachandra, V. K.; Nocera, D. G. *J. Am. Chem. Soc.* **2010**, *132*, 13692-13701.
- (a) Rigsby, M. L.; Mandal, S.; Nam, W.; Spencer, L. C.; Llobet, A.; Stahl, S. S. *Chem. Sci.* **2012**, *3*, 3058-3062. (b) Lai, W.; Cao, R.; Dong, G.; Shaik, S.; Yao, J.; Chen, H. *J. Phys. Chem. Letters* **2012**, *3*, 2315-2319. (c) Leung, C.-F.; Ng, S.-M.; Ko, C.-C.; Man, W.-L.; Wu, J.; Chen, L.; Lau, T.-C. *Energy Environ. Sci.* **2012**, *5*, 7903-7907. (d) Hong, D.; Jung, J.; Park, J.; Yamada, Y.; Suenobu, T.; Lee, Y.-M.; Nam, W.; Fukuzumi, S. *Energy Environ. Sci.* **2012**, *5*, 7606-7616. (e) Wasylenko, D. J.; Palmer, R. D.; Schott, E.; Berlinguette, C. P. *Chem. Commun.* **2012**, *48*, 2107-2109. (f) Gerken, J. B.; McAlpin, J. G.; Chen, J. Y. C.; Rigsby, M. L.; Casey, W. H.; Britt, R. D.; Stahl, S. S. *J. Am. Chem. Soc.* **2011**, *133*, 14431-14442. (g) Luo, J.; Rath, N. P.; Mirica, L. M. *Inorg. Chem.* **2011**, *50*, 6152-6157. (h) Dogutan, D. K.; McGuire, R.; Nocera, D. G. *J. Am. Chem. Soc.* **2011**, *133*, 9178-9180. (i) Shevchenko, D.; Anderlund, M. F.; Thapper, A.; Styring, S. *Energy Environ. Sci.* **2011**, *4*, 1284-1287. (j) Ng G. K-Y; Ziller, J. W.; Borovik, A. S. *Chem. Commun.* **2012**, *48*, 2546-2548.
- (a) Berardi, S.; La Ganga, G.; Natali, M.; Bazzan, I.; Puntoriero, F.; Sartorel, A.; Scandola, F.; Campagna, S.; Bonchio, M. *J. Am. Chem. Soc.* **2012**, *134*, 11104-11107. (b) La Ganga, G.; Puntoriero, F.

- Campagna, S.; Bazzan, I.; Berardi, S.; Bonchio, M.; Sartorel, A.; Natali, M.; Scandola, F. *Faraday Discussions* **2012**, *155*, 177-190. (c) McAlpin, J. G.; Stich, T. A.; Ohlin, C. A.; Surendranath, Y.; Nocera, D. G.; Casey, W. H.; Britt, R. D. *J. Am. Chem. Soc.* **2011**, *133*, 15444-15452. (d) McCool, N. S.; Robinson, D. M.; Sheats, J. E.; Dismukes, G. C. *J. Am. Chem. Soc.* **2011**, *133*, 11446-11449. (e) Symes, M. D.; Lutterman, D. A.; Teets, T. S.; Anderson, B. L.; Breen, J. J.; Nocera, D. G. *ChemSusChem* **2013**, *6*, 65-69.
16. (a) Tueysuez, H.; Hwang, Yun J.; Khan, S. B.; Asiri, Abdullah M.; Yang, P. *Nano Res.* **2013**, *6*, 47-54. (b) Grzelczak, M.; Zhang, J.; Pfrommer, J.; Hartmann, J.; Driess, M.; Antonietti, M.; Wang, X. *ACS Catal.* **2013**, *3*, 383-388. (c) Hu, X. L.; Piccinin, S.; Laio, A.; Fabris, S. *ACS Nano* **2012**, *6*, 10497-10504. (d) Yusuf, S.; Jiao, Feng *ACS Catal.* **2012**, *2*, 2753-2760. (e) Jia, H.; Stark, J.; Zhou, L. Q.; Ling, C.; Sekito, T.; Markin, Z. *RSC Advances* **2012**, *2*, 10874-10881. (f) Klahr, B.; Gimenez, S.; Fabregat-Santiago, F.; Bisquert, J.; Hamann, T. W. *J. Am. Chem. Soc.* **2012**, *134*, 16693-16700. (g) Ahn, H. S.; Tilley, T. D. *Adv. Functional Mater.* **2013**, *23*, 227-233. (h) Zidki, T.; Zhang, L.; Shafirovich, V.; Lyman, S. V. *J. Am. Chem. Soc.* **2012**, *134*, 14275-14278. (i) Xi, L.; Tran, P. D.; Chiam, S. Y.; Bassi, P. S.; Mak, W. F.; Mulmudi, H. K.; Batabyal, S. K.; Barber, J.; Loo, J. S. C.; Wong, L. H. *J. Phys. Chem. C* **2012**, *116*, 13884-13889. (j) Liao, M.; Feng, J.; Luo, W.; Wang, Z.; Zhang, J.; Li, Z.; Yu, T.; Zou, Z. *Adv. Functional Mater.* **2012**, *22*, 3066-3074. (k) Wang, Y.; Wang, Y.; Jiang, R.; Xu, R. *Ind. Eng. Chem. Res.* **2012**, *51*, 9945-9951. (l) Yamada, Y.; Yano, K.; Hong, D.; Fukuzumi, S. *Phys. Chem. Chem. Phys.* **2012**, *14*, 5753-5760. (m) Risch, M.; Shevchenko, D.; Anderlund, M. F.; Styring, S.; Heidkamp, J.; Lange, K. M.; Thapper, A.; Zaharieva, I. *Int. J. Hydrogen Energy* **2012**, *37*, 8878-8888. (n) Risch, M.; Klingan, K.; Ringleb, F.; Chernev, P.; Zaharieva, I.; Fischer, A.; Dau, H. *ChemSusChem* **2012**, *5*, 542-549. (o) Pilli, S. K.; Furtak, T. E.; Brown, L. D.; Deutsch, T. G.; Turner, J. A.; Herring, A. M. *Energy Environ. Sci.* **2011**, *4*, 5028-5034. (p) Jeon, T. H.; Choi, W.; Park, H. *Phys. Chem. Chem. Phys.* **2011**, *13*, 21392-21401. (q) Chou, N. H.; Ross, P. N.; Bell, A. T.; Tilley, T. D. *ChemSusChem* **2011**, *4*, 1566-1569. (r) Wee, T.-L.; Sherman, B. D.; Gust, D.; Moore, A. L.; Moore, T. A.; Liu, Y.; Scaiano, J. C. *J. Am. Chem. Soc.* **2011**, *133*, 16742-16745. (s) Barroso, M.; Cowan, A. J.; Pendlebury, S. R.; Gratzel, M.; Klug, D. R.; Durrant, J. R. *J. Am. Chem. Soc.* **2011**, *133*, 14868-14871. (t) Young, E. R.; Costi, R.; Paydavosi, S.; Nocera, D. G.; Bulovic, V. *Energy Environ. Sci.* **2011**, *4*, 2058-2061. (u) Zhong, D. K.; Cornuz, M.; Sivula, K.; Gratzel, M.; Gamelin, D. R. *Energy Environ. Sci.* **2011**, *4*, 1759-1764. (v) Young, E. R.; Nocera, D. G.; Bulovic, V. *Energy Environ. Sci.* **2010**, *3*, 1726-1728. (w) Risch, M.; Khare, V.; Zaharieva, I.; Gerencser, L.; Chernev, P.; Dau, H. *J. Am. Chem. Soc.* **2009**, *131*, 6936-6937. (x) Zhong, D. K.; Gamelin, D. R. *J. Am. Chem. Soc.* **2010**, *132*, 4202-4207.
17. (a) Yin, Q.; Tan, J. M.; Besson, C.; Geletii, Y. V.; Musaev, D. G.; Kuznetsov, A. E.; Luo, Z.; Hardcastle, K. I.; Hill, C. L. *Science* **2010**, *328*, 342-345. (b) Huang, Z.; Luo, Z.; Geletii, Y. V.; Vickers, J. W.; Yin, Q.; Wu, D.; Hou, Y.; Ding, Y.; Song, J.; Musaev, D. G.; Lian, T.; Hill, C. L. *J. Am. Chem. Soc.* **2011**, *133*, 2068-2071. (c) Huang, Z.; Geletii, Yurii V.; Musaev, D. G.; Hill, C. L.; Lian, T. *Ind. Eng. Chem. Res.* **2012**, *51*, 11850-11859. (d) Zhu, G.; Geletii, Y. V.; Koegerler, P.; Schilder, H.; Song, J.; Lense, S.; Zhao, C.; Hardcastle, K. I.; Musaev, D. G.; Hill, C. L. *Dalton Trans.* **2012**, *41*, 2084-2090. (e) Goberna-Ferron, S.; Vigara, L.; Soriano-Lopez, J.; Galan-Mascaros, J. R. *Inorg. Chem.* **2012**, *51*, 11707-11715. (f) Tanaka, S.; Annaka, M.; Sakai, K. *Chem. Commun.* **2012**, *48*, 1653-1655. (g) Wu, J.; Liao, L.; Yan, W.; Xue, Y.; Sun, Y.; Yan, X.; Chen, Y.; Xie, Y. *ChemSusChem* **2012**, *5*, 1207-1212.
18. (a) Stracke, J. J.; Finke, R. G. *J. Am. Chem. Soc.* **2011**, *133*, 14872-14875. (b) Natali, M.; Berardi, S.; Sartorel, A.; Bonchio, M.; Campagna, S.; Scandola, F. *Chem. Commun.* **2012**, *48*, 8808-8810. (c) Lieb, D.; Zahl, A.; Wilson, E. F.; Streb, C.; Nye, L. C.; Meyer, K.; Ivanovic-Burmazovic, I. *Inorg. Chem.* **2011**, *50*, 9053-9058.
19. (a) Lv, H.; Geletii, Y. V.; Zhao, C.; Vickers, J. W.; Zhu, G.; Luo, Z.; Song, J.; Lian, T.; Musaev, D. G.; Hill, C. L. *Chem. Soc. Rev.* **2012**, *41*, 7572-7589. (b) Mizuno, N.; Kamata, K.; Yamaguchi, K. *Top. Organometallic Chem.* **2011**, *37*, 127-160.
20. Barats, D.; Leitus, G.; Popovitz-Biro, R.; Shimon, L. J. W.; Neumann, R. *Angew. Chem. Int. Ed.* **2008**, *47*, 9908-9912.
21. Pestovsky, O.; Stoian, S.; Bominaar, E. L.; Shan, X.; Münck, E.; Que Jr., L.; Bakac, A. *Angew. Chem. Int. Ed.* **2005**, *44*, 6871-6874.
22. Neumann, R.; Khenkin, A. M. *Chem. Commun.* **1998**, 1967-1968.
23. (a) Jorris, T. L.; Kozik, M.; Casan-Pastor, N.; Domaille, P. J.; Finke, R. G.; Miller, W. K.; Baker, L. C. W. *J. Am. Chem. Soc.* **1987**, *109*, 7402-7408. (b) Khenkin, A. M.; Kumar, D.; Shaik, S.; Neumann, R. *J. Am. Chem. Soc.* **2006**, *128*, 15451-15460.
24. Sanders-Loehr, J.; Wheeler, W. D.; Shiemke, A. K.; Averill, B. A.; Loehr, T. M. *J. Am. Chem. Soc.* **1989**, *111*, 8084-8093.
25. Mayer, J. M. *Acc. Chem. Res.* **2011**, *44*, 36-48.
26. Song, K.-S.; Liu, L.; Guo, Q.-X. *Tetrahedron* **2004**, *60*, 9909-9923.
27. Luo, Y.-R. *Handbook of Bond Dissociation Energies in Organic Compounds*, CRC Press, Boca Raton, 2003.
28. Takahashi, K.; Xing, J.-H.; Hurley, M. D.; Wallington, T. J. *J. Phys. Chem. A* **2010**, *114*, 4224-4231.
29. Buettner, G. R. *Free Radical Biol. Med.* **1987**, *3*, 259-303.
30. Lopez, X.; Carbo, J. J.; Bo, C.; Poblet, J. M. *Chem. Soc. Rev.* **2012**, *41*, 7537-7571.
31. The discrepancy between the experimental and calculated Co-O-Co bond angles precludes the meaningful calculation of the expected Raman frequencies, since they are strongly a function of the bond angle.
32. Wang L.-P.; Van Voorhis T. *J. Phys. Chem. Lett.* **2011**, *2*, 2200-2204.
33. This is a known also for other dicobalt- $\mu$ -oxo compounds *c.f.* Larsen, P. L.; Parolin, T. J.; Powell, D. R.; Hendrich, M. P.; Borovik, A. S. *Angew. Chem. Int. Ed.* **2003**, *42*, 85-89.
34. Lyon, D.K.; Miller, W. K.; Novet, T.; Domaille, P. D.; Evitt, E.; Johnson, D. C.; Finke, R. G. *J. Am. Chem. Soc.* **1991**, *113*, 7209-7221.
35. The disorder in the location of the counter-cations reduces the resolution and Rint. This is not unusual even for stable structures of polyoxometalates *cf.* Ibrahim, M.; Xiang, Y.; Bassil, B. S.; Lan, Y.; Powell, A. K.; de Oliveira, P.; Keita, B.; Ulkörtz, U. *Inorg. Chem.* **2013**, 8399-8408.
36. (a) Lee, C.; Yang, C.; Parr, R. G. *Phys. Rev. B* **1988**, *37*, 785-789. (b) Becke, A. D. *J. Chem. Phys.* **1993**, *98*, 5648-5652. (c) Stephens, P. J.; Devlin, F. J.; Chabalowski, C. F.; Frisch, M. J. *J. Phys. Chem.* **1994**, *98*, 11623-11627 (1994).
37. Hay, P. J.; Wadt, W. R. *J. Chem. Phys.* **1985**, *82*, 270-283.
38. (a) Francl, M. M.; Pietro, W. J.; Hehre, W. J.; Binkley, J. S.; Gordon, M. S.; Defrees, D. J.; Pople, J. A. *J. Chem. Phys.* **1982**, *77*, 3654-3665. (b) Hehre, W. J.; Ditchfield, R.; Pople, J. A. *J. Chem. Phys.* **1972**, *56*, 2257-2261. (c) Hariharan, P. C.; Pople, J. A. *Theor. Chim. Acta* **1973**, *28*, 213-222.
39. Cancès, E.; Mennucci, B.; Tomasi, J. *J. Chem. Phys.* **1997**, *107*, 3032-3041.
40. (a) Perdew, J. P.; Burke, K.; Ernzerhof, M. *Phys. Rev. Lett.* **1996**, *77*, 3865-3868. (b) Adamo C.; Barone, V. *J. Chem. Phys.* **1999**, *110*, 6158-6169.
41. Aquilante, F.; De Vico, L.; Ferré, N.; Ghigo, G.; Malmqvist, P.-Å.; Neogrady, P.; Pedersen, T. B.; Pitonak, M.; Reiher, M.; Roos, B. O.; Serrano-Andrés, L.; Urban, M.; Veryazov, V.; Lindh, R. *J. Comput. Chem.* **2010**, *31*, 224-247.



